Journal of Agrometeorology 3(1&2) : 299 - 317 (June-December 2001)

Numerical simulation of seasonal variation of atmospheric boundary layer processes at Anand

A. N. V. SATYANARAYANA, U. C. MOHANTY*, V. N. LYKOSSOV[1] AND N.V. SAM

Centre for Atmospheric Sciences, I.I.T. New Delhi, India
[1]Institute of Numerical Mathematics, Moscow, Russia

ABSTRACT

Seasonal variation of boundary layer processes using the intensive observational data sets during May, July, September and December, 1997 obtained under LASPEX-97 at Anand (22.4°N, 72.6°E), which represent the pre-monsoon, monsoon, post-monsoon and winter seasons respectively, are presented. For this purpose a one dimensional PBL model with one and half order TKE-epsilon (e- ϵ) closure scheme incorporating interactive soil heat-moisture transportation was employed.

The numerical simulations include the diurnal variations of fluxes of sensible, latent and soil heat, net radiation, soil temperatures, boundary layer height and vertical profiles of potential temperature, mixing ratio, zonal and meridional components of wind. The temporal variation of turbulent kinetic energy is also studied. The model simulations are compared with the available special observational data sets. Overall comparison showed that the model could simulate the boundary layer processes reasonably well.

Key Words: Land Surface Processes, Sensible heat flux, Turbulent Kinetic Energy, PBL, Numerical Simulation

The planetary boundary layer (PBL) is the arena for turbulent exchange of heat, momentum and moisture with the underlying land/ocean surface, which in turn shape the dynamical and thermo-dynamical characteristics of the atmosphere. The variation of fluxes of momentum, heat and moisture in the surface boundary layer and their distribution in the PBL play a crucial role in the energy transport mechanism of the land-ocean-atmospheric system. Proper parameterization of sub-grid scale boundary layer processes is growing in importance in large-scale weather forecasting models (Mahfouf *et al.*, 1987, Stull and Driedonks, 1987 and Holt and Raman, 1988). Soil and vegetation characteristics play vital role in modifying the surface energy balance and thus influence the PBL processes (Mihailovic *et al.*, 1993; Sellers *et al.*, 1986; Noilhan and Planton, 1989; Volodin and Lykossov, 1998). Raman *et al* (1998) have investigated the influence of soil moisture and vegetation variations on simulations of monsoon circulation and rainfall by incorporating a simple land surface parameterization scheme

* *Corresponding Author:* Email: mohanty@cas.iitd.ernet.in.

in a three dimensional, high resolution, regional, nested-grid, atmospheric model. Very few studies are conducted on land surface processes in India and to fill this gap, a multi-institutional Land Surface Processes Experiment (LASPEX-97) funded by Department of Science and Technology, Govt. of India, was conducted by Indian Institute of Tropical Meteorology (IITM) Pune and Gujarat Agriculture University, Anand, over Sabarmati basin area, in 1997. Satyanarayana *et al* (2000) have studied the atmospheric boundary layer characteristics during winter at Anand. In the present study an attempt has been made to simulate the boundary layer characteristics by using a one-dimensional PBL model with the TKE-ϵ (e- ϵ) closure scheme and a simple soil heat and moisture transport model using the LASPEX-97 data sets at Anand during May, July, September and December, 1997 which represent the pre-monsoon, monsoon, post-monsoon and winter seasons respectively.

MATERIALS AND METHODS

Data

In the study, IOP data during 13- 16 May, 13-16 July, 13 -16 September and 14-17 December 1997 at Anand consisting of tower as well as lower troposphere observations are used. The data consists of temperature, wind speed and wind direction at 1, 2, 4 and 8 m height; relative humidity at 2 and 4 m height from 9 m tower and surface pressure. Lower troposphere observations of temperature, dew point temperature, wind speed and wind direction at different pressure levels up to 700 hPa are considered. The data also include Sonic anemometer and Metek anemometer observations on sensible heat flux, and momentum flux; soil type and texture, soil temperature at the surface, 5 cm, 10 cm, 20 cm, 40 cm and 100 cm depth, Soil moisture, incoming solar radiation, reflected incoming solar radiation, soil heat flux at 5 cm depth.

The meteorological tower at Anand was in midst of an agriculture farm located in Gujarat Agriculture University campus. This region is a flat river basin area and is situated in the semi-arid/arid zone of the western part of India. It is nearly homogeneous terrain. Low-level crops were grown during the experimental period. Advection components are found to be small over this area, verified by NCMRWF (National Centre for Medium Range Weather Forecasting) large-scale analyses. The conditions are well suited for applying a one-dimensional/single column model to understand the land-surface processes and boundary layer characteristics at Anand.

Soil heat and moisture transportation model

The exchange processes in the atmospheric surface layer and soil result from a complex interaction among them. This requires a proper parameterization of heat and moisture transfer at the land surface and in the soil, and should be incorporated within the boundary layer models to improve the efficiency of characterizing the boundary-layer processes. A soil heat and moisture transportation scheme has been developed at Centre for Atmospheric Sciences, IIT Delhi and the details of the scheme are given hereunder.

The prognostic equations for soil heat and moisture diffusion can be written as

$$\rho C_p \frac{dT_s}{dt} = \frac{d}{dz} \lambda_T \frac{dT_s}{dz} \quad \ldots (1)$$

$$\frac{dq_S}{dt} = \frac{d}{dz}\lambda_V \frac{dq_S}{dz} \quad \ldots (2)$$

Where

ρ = Soil density (Kgm^{-3});

Cp = soil specific humidity ($J\,kg^{-1}K^{-1}$)

λ_T = Soil heat conductivity coefficient (W/m/K)

λ_V = Moisture diffusivity coefficient

T_s = Temperature of the soil (°K)

q_s = Specific humidity of the soil (gg^{-1})

The soil flux is computed as suggested by Volodin and Lykossov (1998)

$$Soil\ Flux = -\lambda \frac{dT_S}{dZ} \quad \ldots (3)$$

The prescribed values of temperature and specific humidity at the soil bottom are used as the soil lower boundary condition.

One-dimensional PBL model (e-ϵ closure scheme) with soil heat and moisture transport scheme

The interactive soil heat and moisture transport scheme described in the previous section was incorporated in a one-dimensional PBL model with e-ϵ closure scheme to study the impact of the land surface processes in modifying the boundary layer characteristics. In a cartesian co-ordinate system, where the horizontal axes x and y are directed to the east and north respectively, and the vertical axis z is directed upward, the planetary boundary layer equations along with the turbulence closure equations can be written in the following form (Lykossov and Platov, 1992; Kusuma *et al.*, 1996):

$$\frac{\partial u}{\partial t} = -\frac{\partial \overline{u'w'}}{\partial z} + fv + \bar{p}_x/\bar{\rho} \quad \ldots (4)$$

$$\frac{\partial v}{\partial t} = -\frac{\partial \overline{v'w'}}{\partial z} - fu - \bar{p}_y/\bar{\rho} \quad \ldots (5)$$

$$\frac{\partial \theta}{\partial t} + u\bar{\theta}_x + v\bar{\theta}_y = -\frac{\partial \overline{\theta'w'}}{\partial z} + Q_r + Q_f \quad \ldots (6)$$

$$\frac{\partial q}{\partial t} + u\bar{q}_x + v\bar{q}_y = -\frac{\partial \overline{q'w'}}{\partial z} + E_p - C \quad \ldots (7)$$

$$\frac{\partial q_w}{\partial t} + u\bar{q}_{wx} + v\bar{q}_{wy} = -\frac{\partial \overline{q_w'w'}}{\partial z} - E_p + C - P \quad \ldots (8)$$

Where u,v, and w are x, y and z components of the wind velocity, θ is the potential temperature, q is the specific humidity, q_w is the specific liquid-water content, E is turbulent kinetic energy and ρ is dissipation, ϵ is the density of the air - water - water vapour mixture, $(\bar{p}_x,\bar{p}_y).(\bar{\theta}_x,\bar{\theta}_y).(\bar{q}_x,\bar{q}_y)$ are components of horizontal gradients of the pressure, potential temperature, specific humidity and specific liquid-water content in the free atmosphere, Q_r and Q_f are rates of the heat change due to radiation and phase transitions of the water, C and E_p are rates of phase changes: water vapour to liquid water and water to water

vapour, P is the precipitation rate,

$\rho\overline{u'w'}$, $\rho\overline{v'w'}$, $\rho\overline{\theta'w'}$, $\rho\overline{q'w'}$ and $\rho\overline{q'_w w'}$

are the vertical turbulent fluxes of momentum, heat, water vapor and liquid water, f is corilois parameter.

Parameterization of pressure forcing and advection

To compute the pressure gradient in Eq. (4) and (5), the geostrophic wind relationships are used. To compute the horizontal gradients of temperature, the thermal wind relationships are employed (Satyanarayana *et al.*, 2000)

Turbulence closure

In the model, the atmospheric boundary layer is partitioned into two sub-domains: the near surface constant-flux layer ($z \leq h$) (h is the height of constant flux layer) and the free-atmosphere-topped interfacial layer ($h<z \leq H$) (H is the top of the model domain). It is assumed that h and H do not vary in time. In order to calculate vertical turbulent fluxes of momentum, heat and moisture in the interfacial layer, the Boussinesq hypothesis is used. To compute turbulent kinetic energy (E) and dissipation (ϵ), additional prognostic equations are used.

$$\frac{\partial E}{\partial t} = (-\overline{u'w'}\frac{\partial u}{\partial z} + \overline{v'w'}\frac{\partial v}{\partial z} + \frac{g}{\rho}\overline{\rho'w'} + \varepsilon) - \frac{\partial \overline{w'E'}}{\partial z}$$

$$\frac{\partial \varepsilon}{\partial t} = -C_1\frac{\varepsilon}{b}(-\overline{u'w'}\frac{\partial u}{\partial z} + \overline{v'w'}\frac{\partial v}{\partial z} + \frac{g}{\rho}\overline{\rho'w'} + \varepsilon) - \frac{\partial \overline{w'\varepsilon'}}{\partial z}$$

Where , g is acceleration due to gravity, C_1, and b are constants.

Radiation

An important process in the evolution of atmospheric boundary layer and in its interaction with the surface is radiation, which is described by the term Q_r in Eq. 6. Without dwelling on the radiation block of the model, we point out that

$$\rho C_p Q_r = -\frac{\partial(F\downarrow - F\uparrow)}{\partial z}$$

Where F↓ -and F ↑) stand for the total upwelling and down-welling radiative fluxes respectively. The model has both short-wave heating and long wave cooling effects. To calculate the radiative fluxes, the radiation scheme developed by Harshvardhan *et al.* (1987) has been used. Effects of water vapour, ozone and carbon dioxide are included in this parameterization. Additionally, the short-wave radiative flux is influenced by the underlying surface albedo and cloud albedo.

Lower boundary conditions

The lower boundary of the interfacial layer is kept as the maximum height of the constant flux layer. Then, the lower boundary conditions for the prognostic variables at the constant flux layer height, z = h, are as follows:

$$K\frac{\partial u}{\partial z} = C_D\left|\vec{V}_h\right|u_h$$

$$K\frac{\partial v}{\partial z} = C_D\left|\vec{V}_h\right|v_h$$

$$\frac{H_S}{C_P\rho} = K_\theta \frac{\partial\theta}{\partial z} = -C_\theta \left|\vec{V}_h\right| (\theta_h - \theta_s)$$

$$\frac{E_S}{\rho} = K_q \frac{\partial q}{\partial z} = -C_\theta \left|\vec{V}_h\right| (q_h - q_s)$$

Where H_s and LE_s are the sensible and latent heat fluxes at the land surface, the subscript h indicates that the corresponding quantities refer to the upper boundary of the constant flux layer, the subscript s refers to the quantities determined at the air-soil interface. In eq. (12 to 15) we have used to notation $\vec{V} = (u, v)$. The surface layer is treated in the light of Monin and Obukhov similarity theory (Satyanarayana *et al.*, 2000).

Soil heat and moisture transport Scheme

To compute the surface temperature, Ts and specific humidity, q_s, the surface energy and water budget equations are used. The details of the soil heat and moisture transport scheme are explained earlier in the manuscript.

Upper boundary conditions

The maximum height of the turbulent boundary layer (top of the PBL) is chosen as the upper boundary. At the top of the boundary layer, the wind speeds, the potential temperature and the moisture attain the observed values at that height. The TKE flux and dissipation flux are assumed to vanish at that height.

Initial conditions

The initial conditions prepared for the study are i) 00 UTC RS/RW data of 13 May 1997, ii) 00 UTC RS/RW data of 13 July 1997, iii) 03 UTC RS/RW data of 13 September 1997 and iv) 00 UTC RS/RW data of 14 December 1997 at Anand station. For all the above cases, the model is integrated for 72 hours with time step of 600 seconds.

RESULTS AND DISCUSSION

The observed profiles of zonal and meridional wind components, potential temperature and specific humidity obtained from RS/RW observations, linearly interpolated in the vertical at every 50 m interval up to 2000 m were used to compare with the simulations. First 12 hours of model simulations are not considered for the analysis as it was due to the spin up time of the model. The results pertain only to IOP period in a month.

The vertical profiles of model simulations and observations of zonal and meridional wind components, potential temperature and specific humidity on 14 May at 06 UTC; 14 July at 03 UTC; 14 September at 06 UTC; 14 December at 00 UTC are depicted in Fig. 1 - 4. Model was able to simulate the stable stratification (Fig. 3c and 4c) and unstable stratification (Fig. 1c) very well. But during monsoon period the stable stratification in the lower levels is not simulated reasonably. Except during pre and post monsoon periods, the model could simulate the specific humidity reasonably well. In general, the model simulated the zonal, meridional wind components reasonably well.

Model predictions of diurnal and day-to-day variation of net radiation flux along with the observations during 00 UTC of 13 to 00 UTC of 16 May; 00 UTC of 13 to 00 UTC of 16 July; 03 UTC of 13 to 03 UTC of 16 September and 00 UTC of 14 to 00 UTC of 17 December are presented in Fig. 5 The

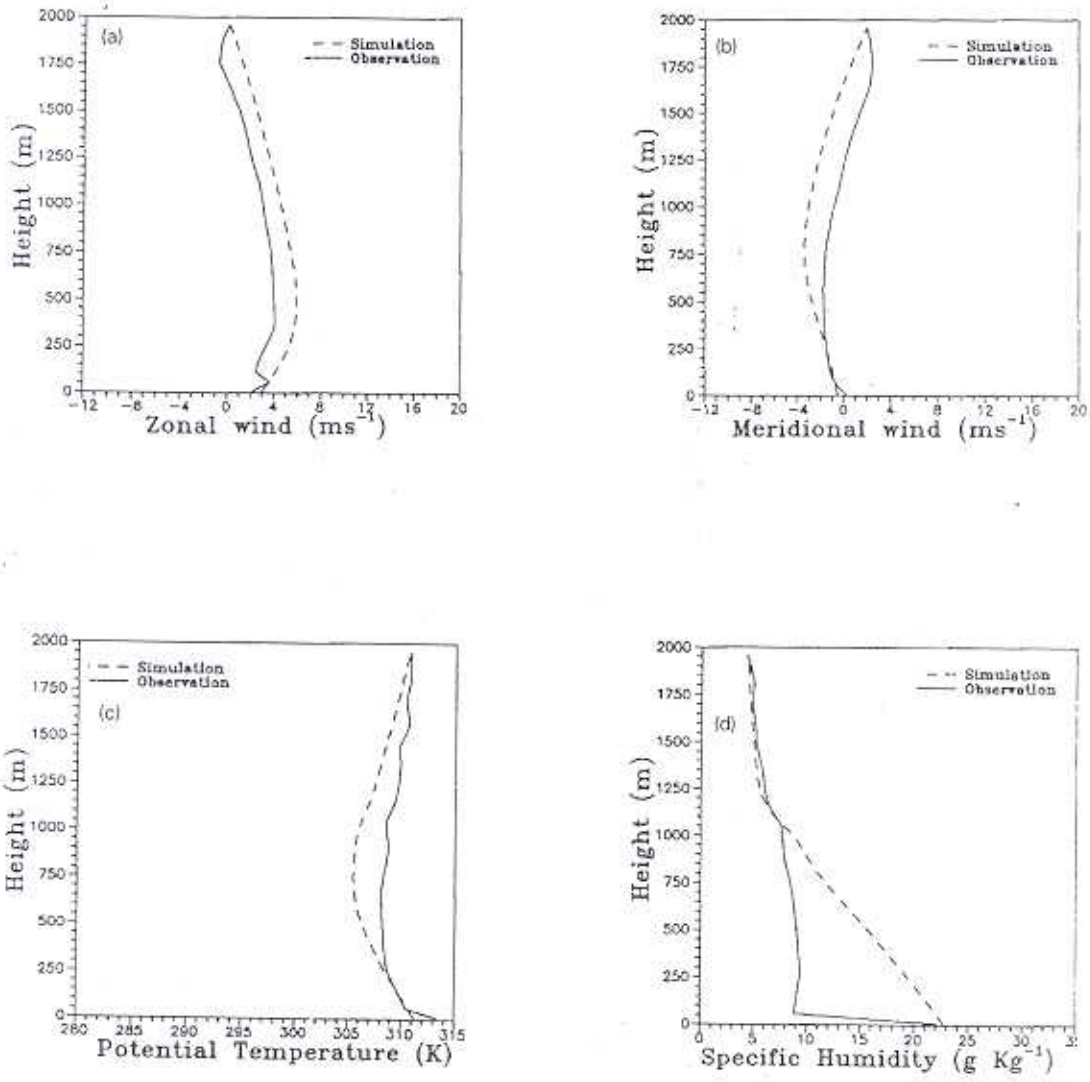

Fig. 1 : Observed and simulated vertical profiles of a) zonal wind (ms^{-1}), b) meridional wind (ms^{-1}), c) potential temperature (K) and d) specific humidity (g kg^{-1}) at 06 UTC on 14 May 1997 at Anand

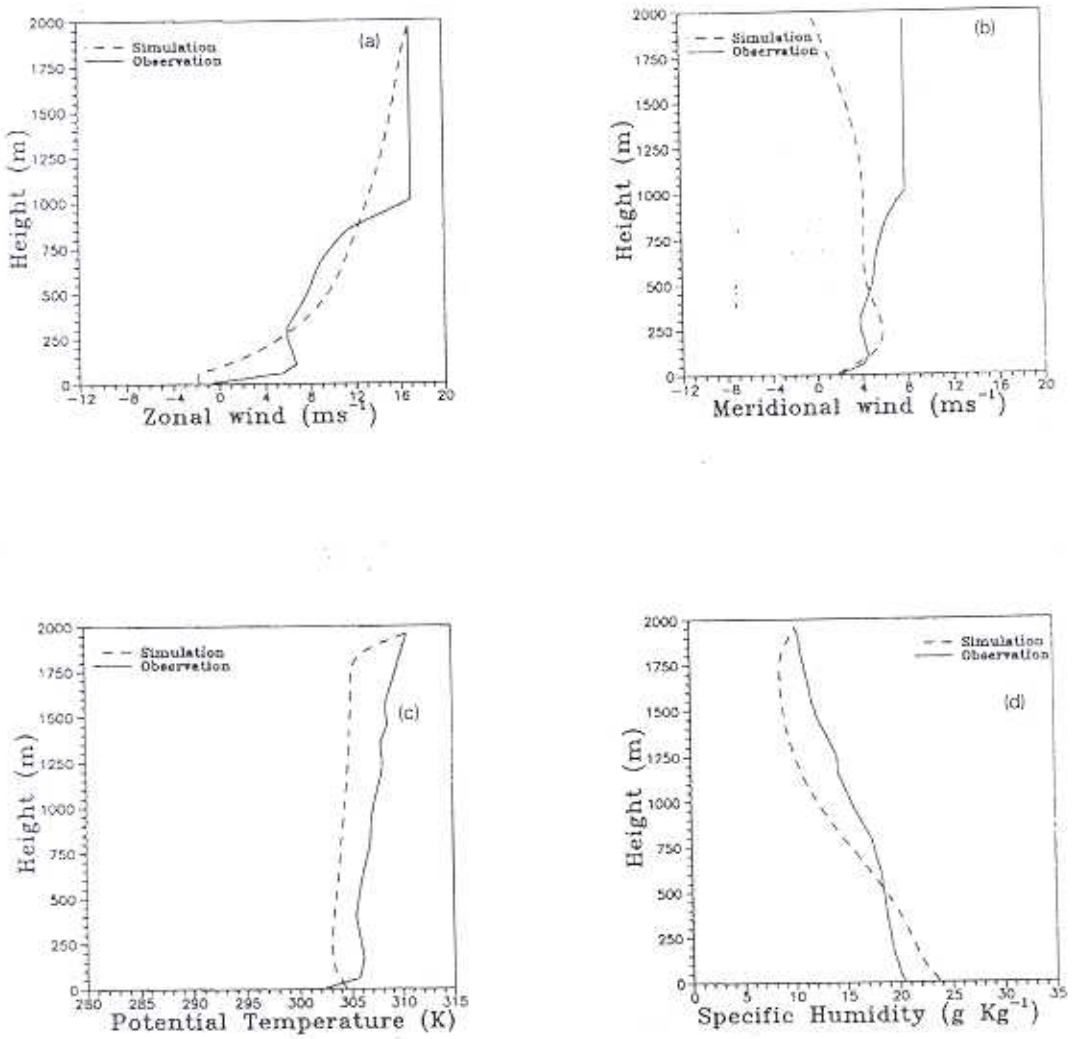

Fig. 2 : Observed and simulated vertical profiles of a) zonal wind (ms^{-1}), b) meridional wind (ms^{-1}), c) potential temperature (K) and d) specific humidity (g kg^{-1}) at 03 UTC on 14 July 1997 at Anand

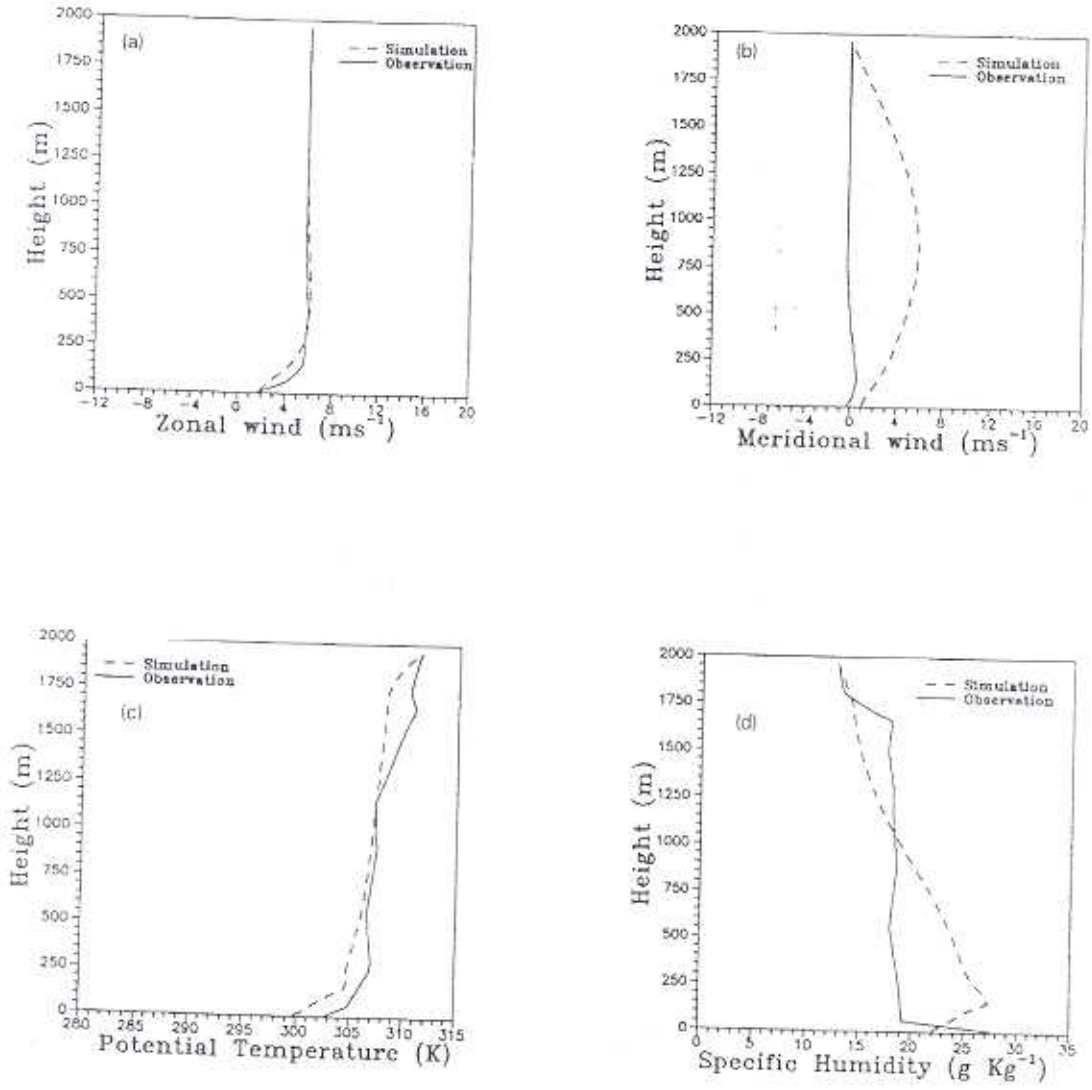

Fig. 3 : Observed and simulated vertical profiles of a) zonal wind (ms^{-1}), b) meridional wind (ms^{-1}), c) potential temperature (K) and d) specific humidity (g kg^{-1}) at 06 UTC on 14 September 1997 at Anand

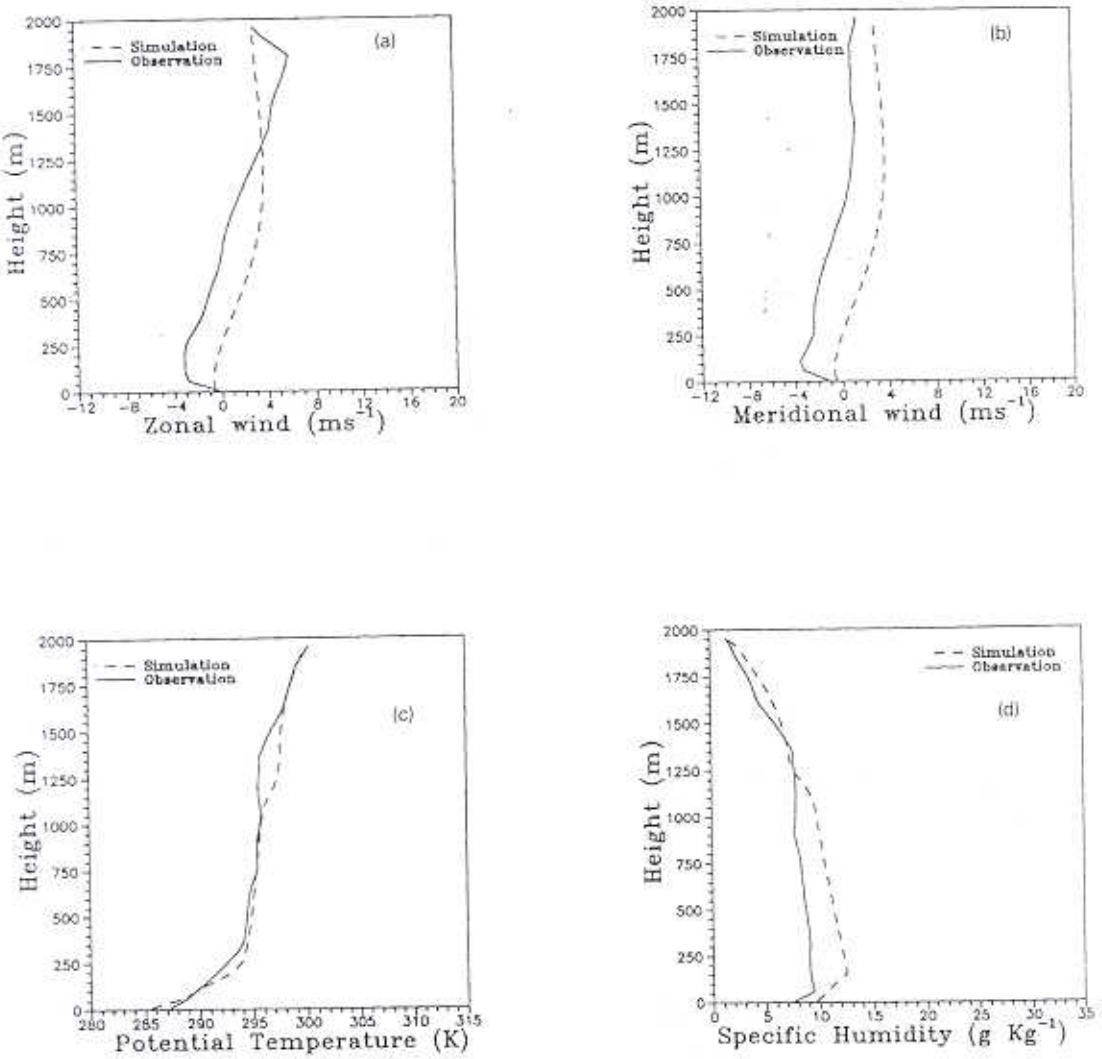

Fig. 4 : Observed and simulated vertical profiles of a) zonal wind (ms^{-1}), b) meridional wind (ms^{-1}), c) potential temperature (K) and d) specific humidity ($g\ kg^{-1}$) at 00 UTC on 14 December 1997 at Anand

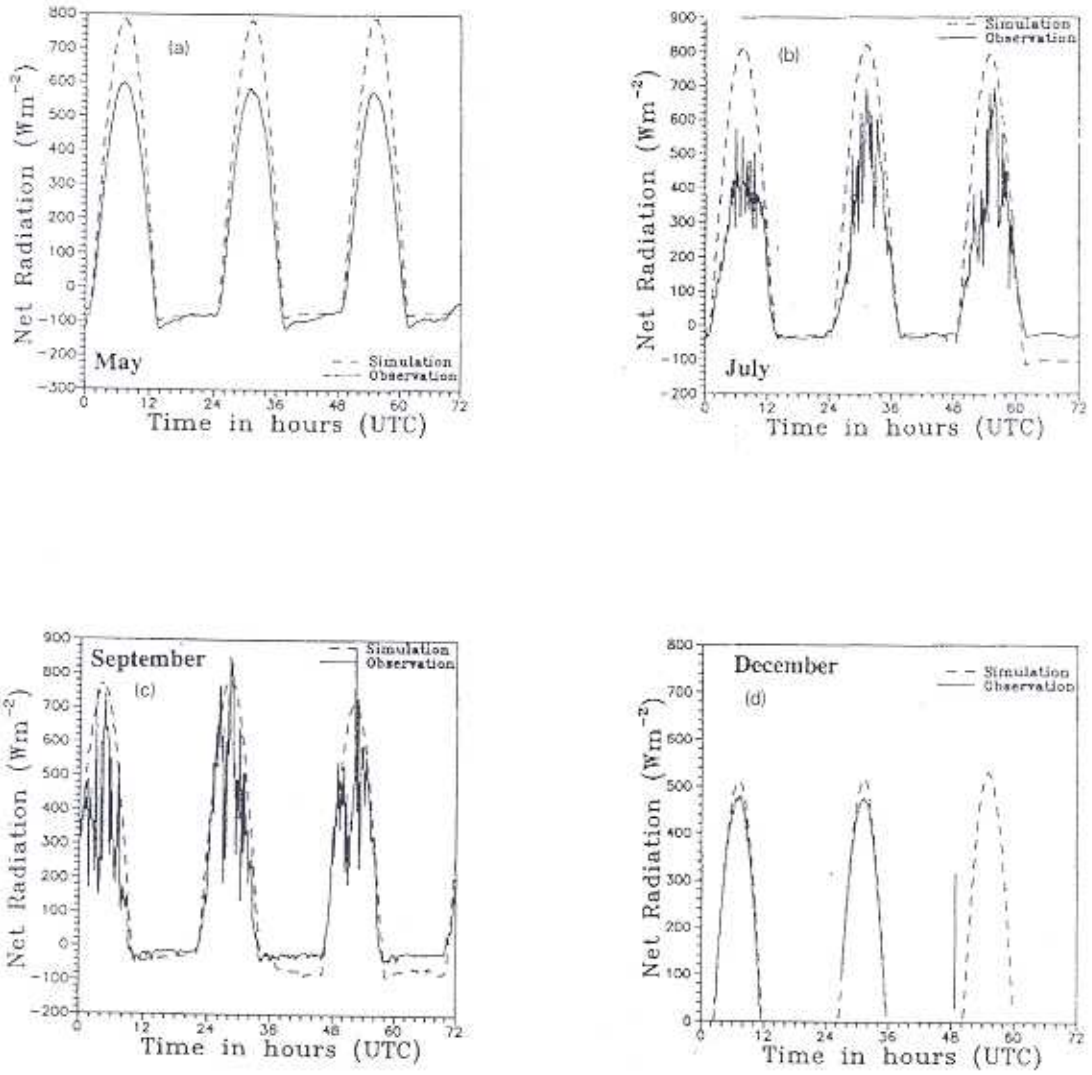

Fig. 5 : Diurnal and day-to-day variation of net radiation flux (Wm^{-2}) along with the observations during a) 00 UTC of 13 to 00 UTC of 16 May 1997, b) 00 UTC of 13 to 00 UTC of 16 July 1997, c) 03 UTC of 13 to 03 UTC of 16 September 1997 and d) 00 UTC of 14 to 00 UTC of 17 December 1997 at Anand

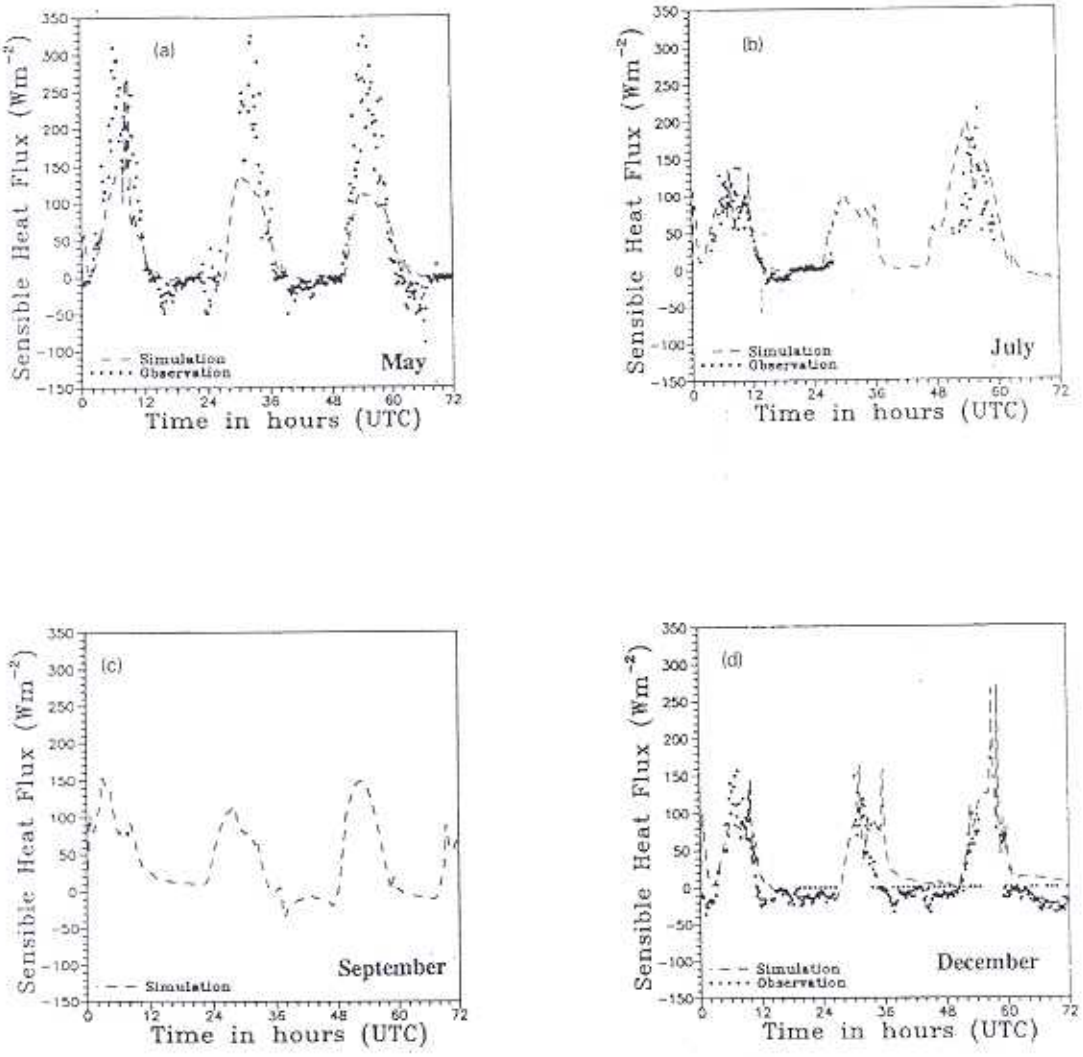

Fig. 6 : Diurnal and day-to-day variation of sensible heat flux (Wm^{-2}) along with the observations during a) 00 UTC of 13 to 00 UTC of 16 May 1997, b) 00 UTC of 13 to 00 UTC of 16 July 1997, c) 03 UTC of 13 to 03 UTC of 16 September 1997 and d) 00 UTC of 14 to 00 UTC of 17 December 1997 at Anand

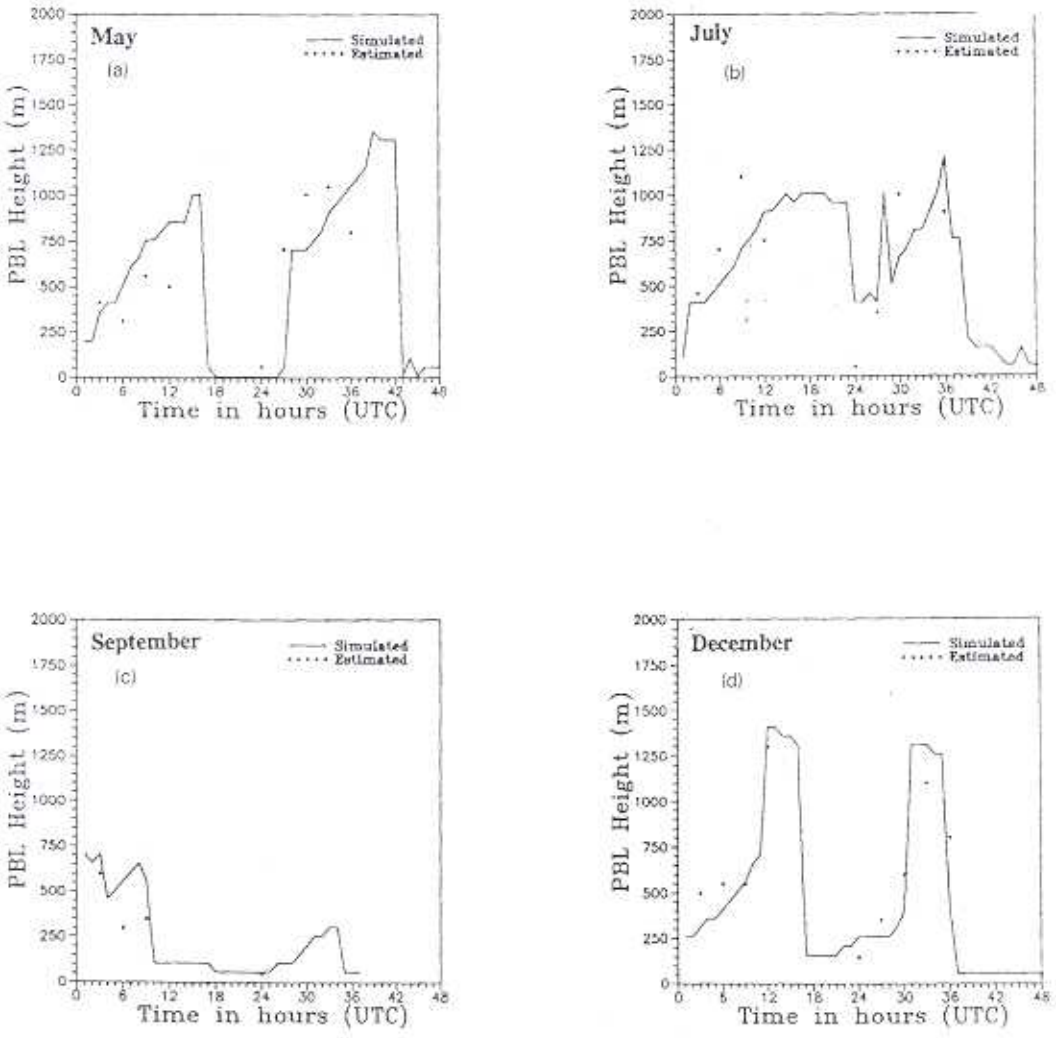

Fig. 7 : Diurnal and day-to-day variation of boundary layer height (m) along with the estimated values during a) 00 UTC of 13 to 00 UTC of 16 May 1997, b) 00 UTC of 13 to 00 UTC of 16 July 1997, c) 03 UTC of 13 to 03 UTC of 16 September 1997 and d) 00 UTC of 14 to 00 UTC of 17 December 1997 at Anandas e) but simulations at Anand

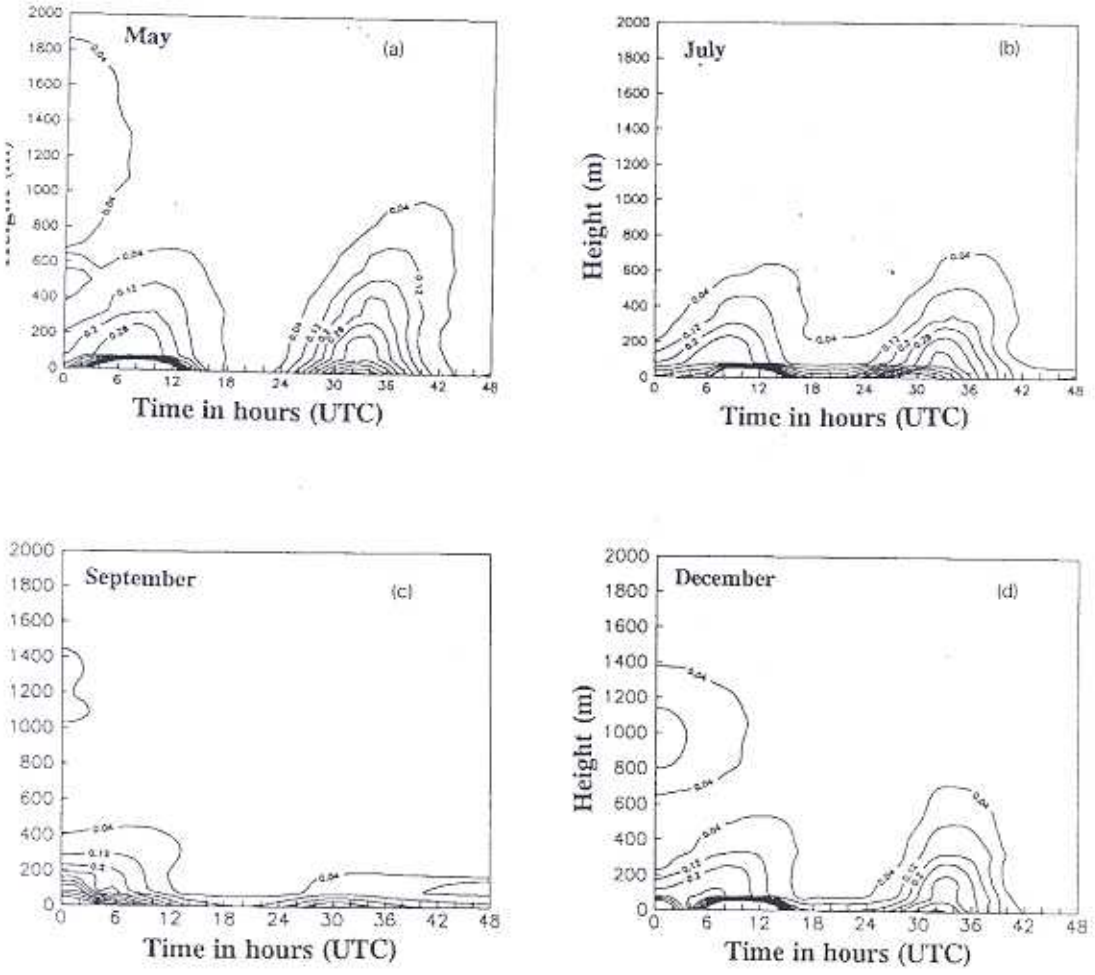

Fig. 8 : Time evolution of turbulent Kinetic Energy (m^2s^{-2}) during a) 00 UTC of 13 to 00 UTC of 15 May 1997, b) 00 UTC of 13 to 00 UTC of 15 July 1997, c) 03 UTC of 13 to 03 UTC of 15 September 1997 and d) 00 UTC of 14 to 00 UTC of 16 December 1997

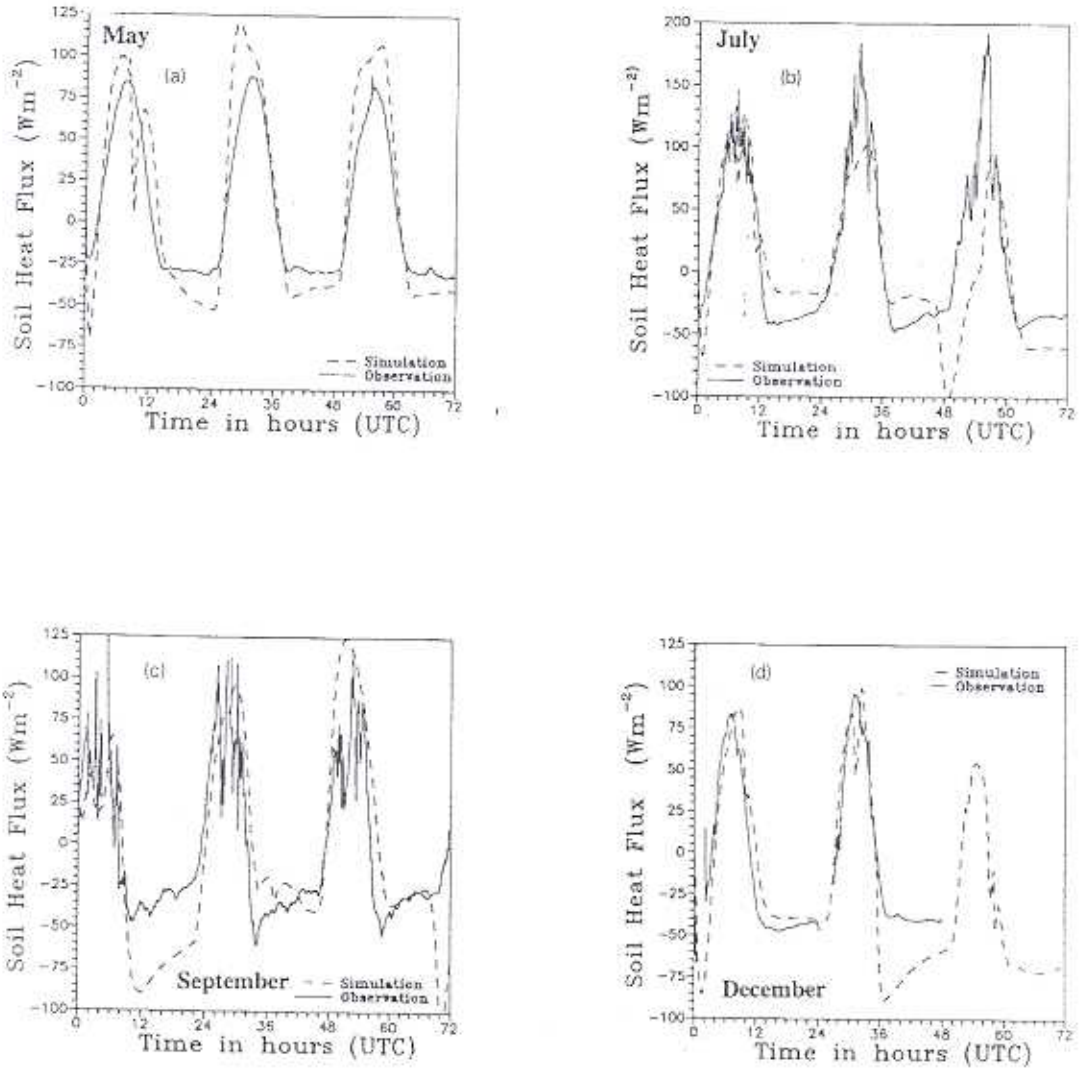

Fig. 9 : Diurnal and day-to-day variation of soil heat flux (Wm^{-2}) along with the observations during a) 00 UTC of 13 to 00 UTC of 16 May 1997, b) 00 UTC of 13 to 00 UTC of 16 July 1997, c) 03 UTC of 13 to 03 UTC of 16 September 1997 and d) 00 UTC of 14 to 00 UTC of 17 December 1997 at Anand

model over predicted the flux during May and July where as not much variation is noticed during September and December. During May a deviation of around 200 Wm^{-2} is seen between observations and simulations. As expected, relatively less net radiation flux is observed during July and December in comparison with May and September.

The model simulations of sensible heat flux along with the observations during 00 UTC of 13 to 00 UTC of 16 May; 00 UTC of 13 to 00 UTC of 16 July; 03 UTC of 13 to 03 UTC of 16 September and 00 UTC of 14 to 00 UTC of 17 December are presented in Fig. 6. Due to the non-availability of the direct measurements of the sensible heat flux during September (Fig. 6c), only model simulations are presented. The model predictions show clear-cut diurnal as well as day-to-day variation during all the four seasons. The observed values are plotted whenever they were available. In general, the model simulations fairly agree with the observations. During May, the model under-predicted the maximum value of the flux where as during July and December they are matching well with the observations. From the observations one can see the clear-cut seasonal variation. During May a maximum flux around 330 Wm^{-2} is observed where as during July and December the maximum is between 150 - 200 Wm^{-2}.

Model predictions of diurnal and day-to-day variation of boundary layer height along with the estimated values during 00 UTC of 13 to 00 UTC of 16 May; 00 UTC of 13 to 00 UTC of 16 July; 03 UTC of 13 to 03 UTC of 16 September and 00 UTC of 14 to 00 UTC of 17 December are presented in Fig. 7 Boundary layer height is estimated using the observed thermodynamic profiles. These estimated values are overlaid on the simulated boundary layer height curve. The height at which the turbulent kinetic energy ceases is taken as the PBL height. The maximum simulated boundary layer height is seen during the month of May is around 1500 m. In case of July and December it ranges between 1250 - 1440m. Diurnal as well as day-to-day variation of boundary layer height is seen during May, July and December. No specific variation is found during September. The model simulations of boundary layer height are in good agreement with the estimated values.

The temporal evolution of turbulent kinetic energy (TKE) during 00 UTC of 13 to 00 UTC of 15 May 1997; 00 UTC of 13 to 00 UTC of 15 July 1997; 03 UTC of 13 to 03 UTC of 15 September 1997 and 00 UTC of 14 to 00 UTC of 16 December 1997 are presented in Fig. 8. Higher values of TKE are noticed during May followed by July, December and less magnitude is noticed in September. During May a maximum TKE of 0.6 $m^{-2}s^{-2}$ is noticed. During May, July and December diurnal variation of TKE is noticed except during September.

The model simulations of soil heat flux along with the observations during 00 UTC of 13 to 00 UTC of 16 May; 00 UTC of 13 to 00 UTC of 16 July; 03 UTC of 13 to 03 UTC of 16 September and 00 UTC of 14 to 00 UTC of 17 December are presented in Fig. 9. During May, the model over-predicted the soil heat flux and the deviation from the maximum value is around 20 Wm^{-2}. A maximum Flux of 90 Wm^{-2} is noticed in the observations. During July, the model under-predicted the flux. A maximum flux 195 Wm^{-2} is seen in the observations. The occurrence of maximum value of the soil heat flux is simulated well.

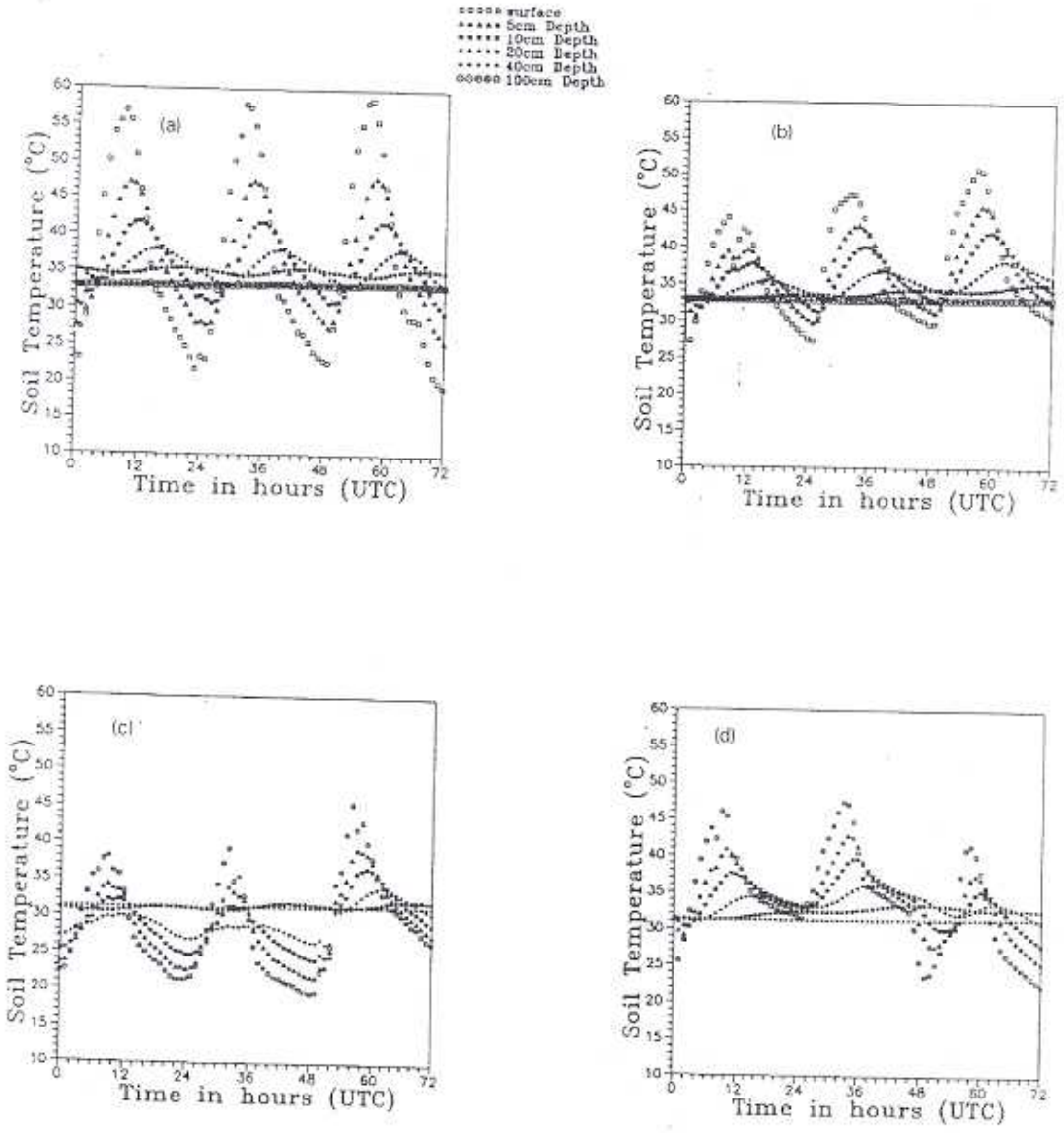

Fig. 10 : Diurnal and day-to-day variation of soil temperature (° C) at different depths during a) 00 UTC of 13 to 00 UTC of 16 May 1997 (observations), b) same as a) but simulations, c) 00 UTC of 13 to 00 UTC of 16 July 1997 (observations), d) same as c) but simulations at Anand

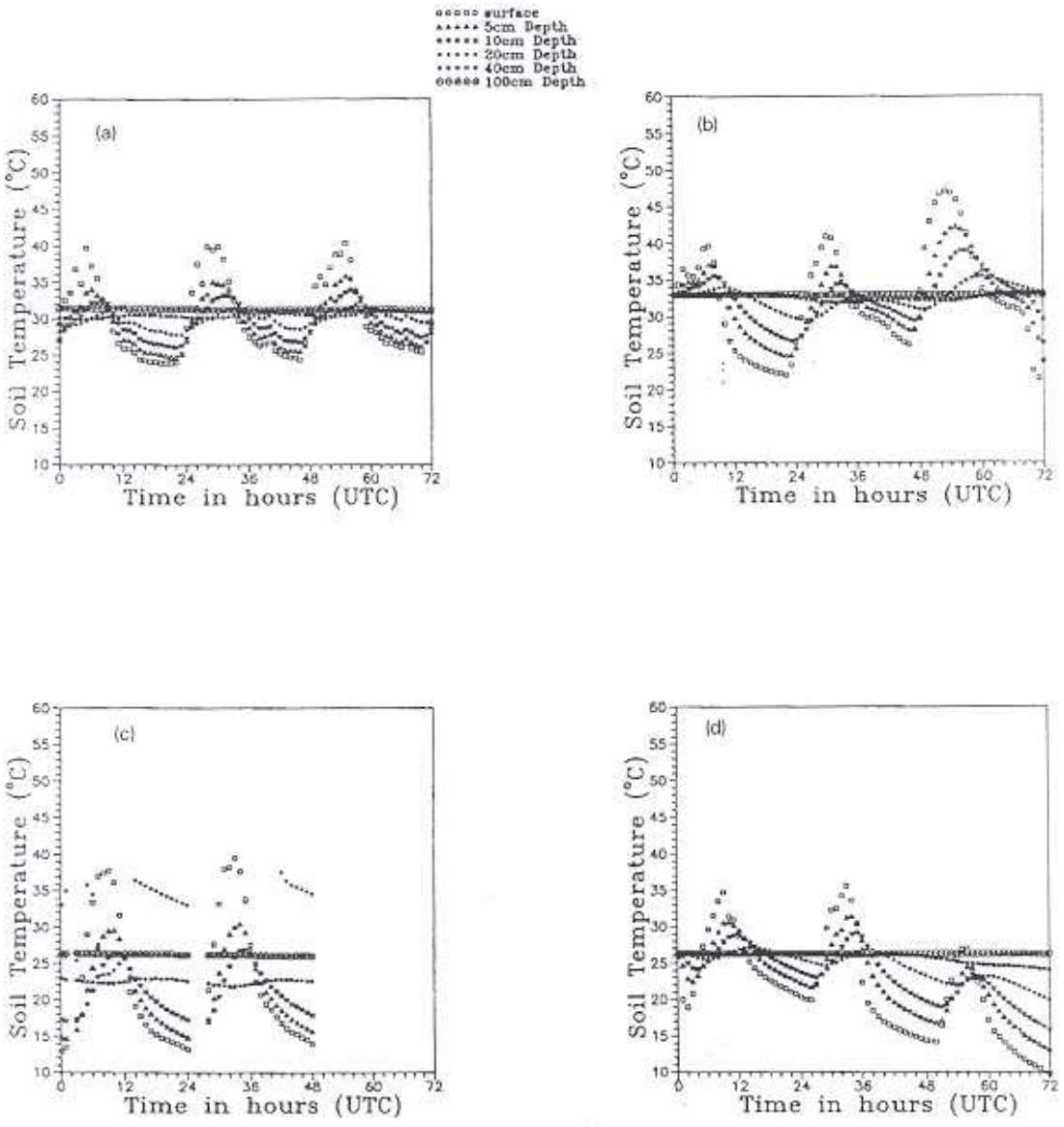

Fig. 11 : Diurnal and day-to-day variation of soil temperature (o C) at different depths during a) 03 UTC of 13 to 03 UTC of 16 September 1997 (observations), b) same as a) but simulations, c) 00 UTC of 14 to 00 UTC of 17 December 1997 (observations), d) same

During September as well as December, the model simulations are in fair agreement with the observations. During September a maximum flux of 120 Wm^{-2} is observed where as in December it is 90 Wm^{-2}. Higher values of soil heat flux are noticed in July case.

Fig. 10 - 11 depict the diurnal, day-to-day, seasonal variation of soil temperature during May, July, September and December 1997. The model simulations show clear-cut diurnal variation as noticed in the observations. The model over-predicted the maximum soil temperature during July where as it under-predicted during May. But during September and December simulations are in good agreement with the observations. A maximum soil temperature ranging between 57-59 °C is observed at the surface in the month of May. During July, September and December the maximum is ranging between 37-45 °C. In all the four cases the occurrence of the maximum value of soil temperature is matching well with the observations.

CONCLUSIONS

From the results of the numerical simulations carried in this study the following broad conclusions may be drawn.

Model simulations of sensible heat flux are in good agreement with observations in May, July and December and reveal a good synchronization of the maxima and minima with the observations. Simulated latent heat flux for May, July, September and December compared reasonably well with the estimated values. Net-radiation flux is over estimated in May and July. Variation of the energy fluxes is simulated reasonably well. Diurnal variation of PBL height is seen in May and December and no such variation is noticed in July and September. Estimated and simulated PBL height values are in good agreement in all four seasons. Diurnal variation of soil temperature at different depths is simulated reasonably well on comparing with the observations. More TKE evolution is seen in May due to Buoyancy generation; mechanical generation of TKE is seen in July and to some extent in December. No specific temporal variation of TKE is found in September. Vertical profiles of zonal wind and meridional wind components, potential temperature and specific humidity during all four seasons are in good agreement with the observations.

ACKNOWLEDGEMENTS

The authors gratefully acknowledge the Department of Science and Technology, Govt. of India for the financial support to carryout the study. The authors also thank Dr. G.B. Pant, Director, IITM, Pune and BL&LSPS Group of IITM and India Meteorological Department (IMD), New Delhi for providing the necessary data sets.

REFERENCES

Charney, J. G., Quiste, W. J., Chow, S.H. and Korhefield. 1977. A comparative study of the effects of albedo change in drought in semi-arid region. *J. Atmos. Sci.*, 34 : 1366-1385.

Harshavardhan, Roger, D., Randall, D. A. and Corsetti, T. G. 1987. A Fast Radiation Parameterization for Atmospheric General Circulation Models. *J. Geophys. Res.*, 92 : 1009-1016.

Kusuma, G. Rao, Lykossov, V. N., Prabhu, A., Sridhar, S. and Tonkacheyev, E. 1996. The mean and Turbulence Structure

Simulation of the Monsoon Trough Boundary Layer using a One-Dimensional Model with e-l and e-e closures. *Proc. Indian Acad. Sci. (Earth Planet. Sci.).*, 105:227-260.

Lykossov, V. N. and Platov, G. A. 1992. A Numerical model of interaction between atmospheric and oceanic boundary layers. *Russ. J. Numer. Anal. Math. Modelling*, 7 : 419-440.

Mahfouf, J. F., Richard, E., Mascart, P., Nickerson, E. C. and Rosset, R. 1987. A comparative study of various parameterizations of the planetary boundary layer in numerical mesoscale model. *J. Climate Appl. Meteorol.*, 26:1671-1695.

Mohailovic, D. T., Pielke, R. A., Rajkovic, B., Lee, T. J. and Jeftic, M. 1993. A resistance representation of schemes for evaporation from bare and partly plant covered surfaces for use in atmospheric models. *J. Appl. Meteorol.*, 32:1038-1054.

Mintz, Y. 1984. The sensitivity of numerically simulated climates to land surface boundary conditions. The Global Change, (ed.) J. T. Houghton, Cambridge University press, 79-105.

Noilhan, J. and Planton, S. 1989. A simple parameterization of land surface processes for meteorological models. *Mon. Wea. Rev.*, 117:536-549.

Raman, S., Mohanty, U.C., Reddy, N.C., Alapaty, K. and Madala, R.V. 1998. Numerical simulation of the sensitivity of summer monsoon circulation and rainfall over India to land surface processes. *Pure Appl. Geophys.*, 152:781-809.

Satyanarayana, A. N. V., Lykossov, V. N., and Mohanty, U. C. 2000. A study on atmospheric boundary layer characteristics at Anand, India using LSP experimental data sets. *Bound. Layer Meteorol.*, 96:393-419.

Sellers, P. J., Randall, D. A., Collatz, G. J., Berry, J. A., Field, C. B., Dazlich, D. A., Zhang, C., Collelo, G. D., and Bounoua, L. 1996. A revised land surface parameterization (SiB2) for atmospheric GCMs. Part 1. Model formulation. *J. Climate.*, 9: 676-705.

Stull, R. B. and A. G. M. Driedonks. 1987. Applications of the transilient turbulent parameterization to atmospheric boundary layer simulations. *Bound. Layer Meteorol.*, 40:209-239.

Teddy, Holt and Sethu Raman. 1988. A review of comparative evaluation of multilevel boundary layer parameterizations for first-order and turbulent kinetic energy closure schemes. *Rev. Geophys.*, 26: 761-780.

Volodin, E. M. and Lykossov, V. N. 1998. Parameterization of heat and moisture transfer in the soil-vegetation system for use in atmospheric general circulation model: 1. Formulation and simulations based on local observational data. *Izvestiya, Atmos. Ocean Phy.*, 34: 453-465.